Constitutive Modeling of Skeletal Muscle Tissue with an Explicit Strain-Energy Function

G.M. Odegard
T.L. Haut Donahue

Department of Mechanical Engineering – Engineering Mechanics
Michigan Technological University
1400 Townsend Drive
Houghton, MI 49931

D.A. Morrow
K.R. Kaufman[*]

Department of Orthopedic Surgery
Mayo Clinic/Mayo Foundation
200 First St. SW
Rochester, MN 55905

Abstract

While much work has previously been done in the modeling of skeletal muscle, no model has, to date, been developed that describes the mechanical behavior with an explicit strain-energy function associated with the active response of skeletal muscle tissue. A model is presented herein that has been developed to accommodate this design consideration using a robust dynamical approach. The model shows excellent agreement with a previously published model of both the active and passive length-tension properties of skeletal muscle.

Keywords: Hyperelasticity, Transverse isotropy, Biomechanics, Length-tension relationships, Strain energy density

---

[*] Corresponding author. Email:Kaufman.Kenton@mayo.edu; phone: (507)284-2262

Notation

a_1, a_2, a_{12}	Material constants
b_1, b_2	Material constants
$\mathbf{C}$	Right Cauchy-Green deformation tensor
$\mathbf{E}$	Green strain tensor
$\mathbf{F}$	Deformation gradient tensor
e	orthogonal basis set
$\mathbf{e}_1, \mathbf{e}_2, \mathbf{e}_3$	Basis vectors
$\mathbf{I}$	Identity tensor
J	Jacobian
J_4	Scalar invariant
J_4^0	Value of J_4 for the optimized cross-bridging condition
k	Material constant
L_1, L_2	Scalar invariants
M	Activation stress factor
$\tilde{\mathbf{M}}$	Weighted structural tensor
$\mathbf{m}_1$	Fiber axis vector
$\mathbf{M}_1, \mathbf{M}_2, \mathbf{M}_3$	Structural tensors
p	Langrange multiplier
q	Activation parameter
$\mathbf{S}$	Second Piola-Kirchhoff stress tensor
$\mathbf{S}^a$	Second Piola-Kirchhoff stress for active response
$\mathbf{S}_J^a$	Active second Piola-Kirchhoff stress tensor for the Jenkyn model
$\mathbf{S}^p$	Second Piola-Kirchhoff stress for passive response
S_{11}^J	Longitudinal component of total stress for the Jenkyn model
SF	Specific muscle tension constant
U	Instantaneous potential energy
w_1, w_2, w_3	Weighting factors
X	Material point in $\mathcal{R}$
$\mathbf{x}$	Spatial position vector
$\mathbf{X}$	Material position vector
α	Material constant
β	Material constant
χ	Motion of $\mathcal{R}$
ϕ	Actin/myosin overlap parameter
γ	Material constant
η	Entropy density
λ_1	Longitudinal deformation magnitude
λ_2	Transverse deformation magnitude
λ_3	Shear deformation magnitude
μ	Material constant
θ	Absolute temperature

$\hat{\Psi}$	Response function for the strain-energy density
Ψ_a	Strain-energy density for active response
Ψ_p	Strain-energy density for passive response
$\hat{\Psi}^J$	Passive strain-energy density from Jenkyn model

Introduction

The main functions of the human musculoskeletal system are to sustain loads and provide mobility. Bones and joints themselves cannot produce movement; skeletal muscles provide the ability to move. Knowledge of muscle forces during given activities can provide insight into muscle mechanics, muscle physiology, musculoskeletal mechanics, neurophysiology, and motor control. However, currently available methods for clinical examination or instrumented strength testing only provide information regarding muscle groups. Musculoskeletal models are typically needed to calculate individual muscle forces. Mathematical models of muscle have evolved over the past century. Blix [1] observed that muscle force varies with sarcomere length. Hill created a mathematical model that described the velocity-force characteristics of muscle force generation [2]. Numerous investigators have used Hill-type muscle models to predict individual muscle forces [3-6]. However, these models do not account for mechanical equilibrium in the muscle [7] or curvature of muscle during contraction.

More recently, continuum-mechanics muscle models have started to emerge to address these deficiencies. Continuum modeling allows for the prediction of stresses in the three-dimensional space occupied by the muscle. As a result, the continuum-mechanics approach can be used in conjunction with the finite element method to accurately predict muscle forces. A limited number of two-dimensional [8, 9] and three-dimensional models [10-14] have been proposed. These models predict the stress associated with skeletal muscle for given levels of deformation and activation. However, a constitutive model has not yet been developed that explicitly states the strain energy associated with the active response for skeletal muscle tissue. Current models have strain-energy density formulations that are defined as derivatives with respect to imposed strains. Such a formulation requires that the strain energy be recalculated for any variations in the deformations to be studied. Having an explicit strain-energy density formulation is required for establishing a dynamical framework that can be used to directly calculate the strain energy and internal stresses of muscle tissue, and ultimately describe muscle behavior under a wide range of conditions.

Skeletal muscle is composed of fiber-shaped fascicles that are aligned as shown in Figure 1. The fascicles are, in turn, composed of muscle fibers which are built from myofibrils composed of sarcomeres arranged in series. Like the fascicles, the muscle fibers and myofibrils are aligned along the fiber axis of the muscle tissue. Each sarcomere contains overlapping myosin and actin filaments. Passive force production occurs when a muscle has been stretched from its resting length (Fig. 2) and is largely attributable to the extracellular matrix. This force increases exponentially with relative elongation and will tend to restore the muscle to its resting length once released. Active force production occurs when skeletal muscle activation causes overlapping actin and myosin filaments to interact via cross-bridging, resulting in muscle contraction. As shown in Figure 2, an optimal length exists where there is a sufficient amount of overlap to provide for maximal force generation. Any change in the length of the sarcomere from this optimal length will reduce the overlap available for cross-bridging and therefore reduce the achievable load. At increased sarcomere lengths, however, the passive forces combine to offset the decreasing active force production, resulting in increased total force production.
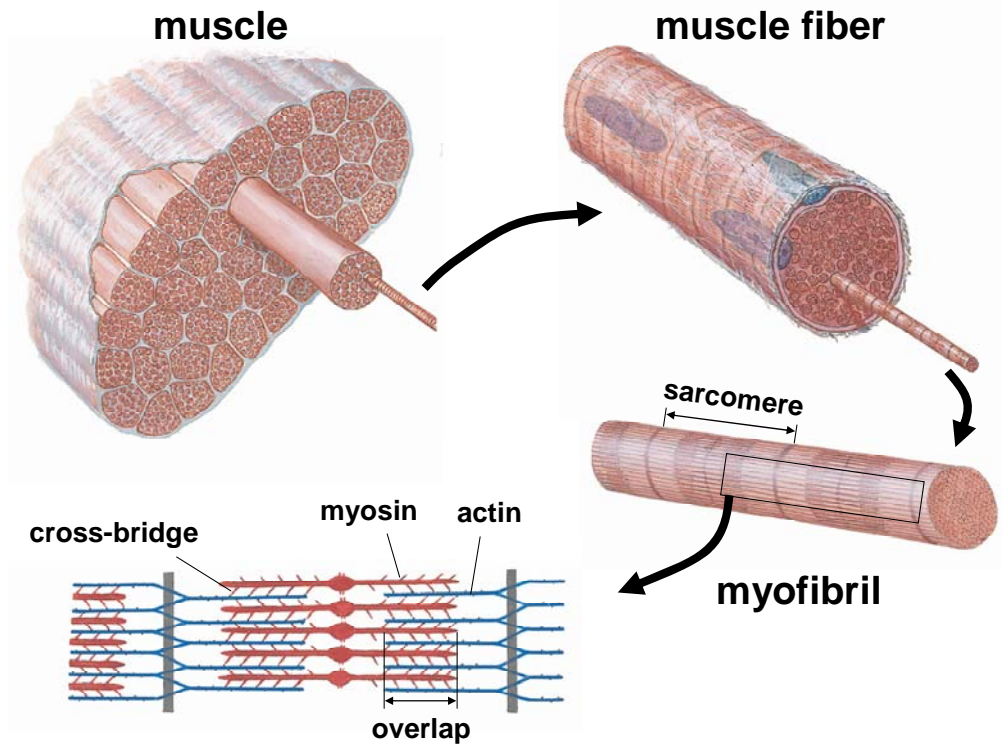
Figure 1. Multiple scale levels of skeletal muscle tissue (Netter medical illustration used with permission of Elsevier. All rights reserved.)
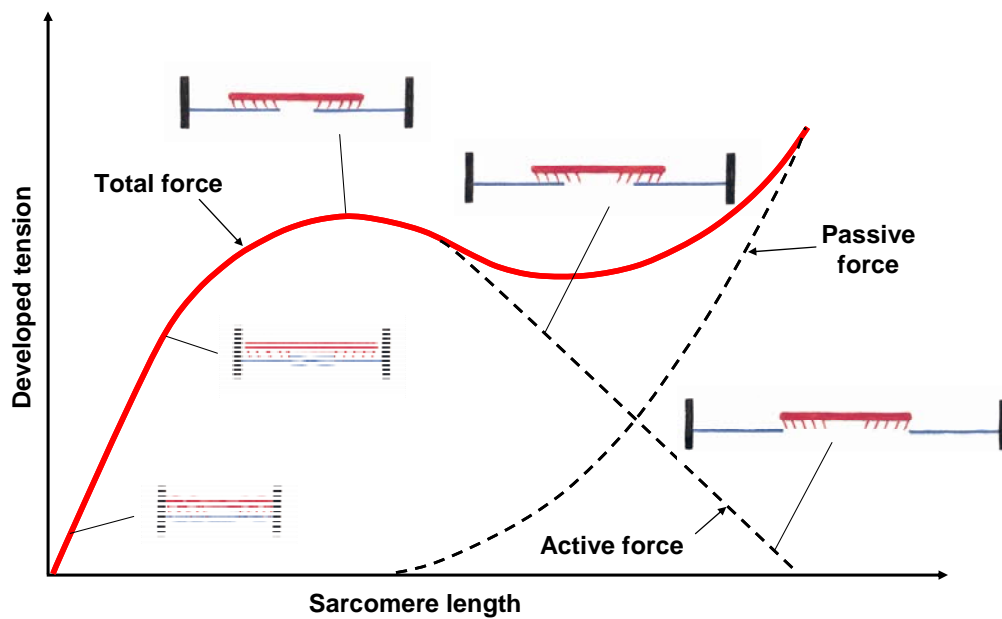

Figure 2. Tension-length relationship of a sarcomere (Netter medical illustration used with permission of Elsevier. All rights reserved.)

It has been reported that skeletal muscle tissue exhibits the same mechanical behavior on both the muscle fiber- and sarcomere-associated length scales [3]. Therefore, for the modeling of mechanical behavior, skeletal muscle tissue can be modeled as a continuous and homogenous effective continuum with mathematically-defined properties and symmetry on multiple length-scale levels. It has been further suggested that muscle tissue is incompressible [15, 16] and exhibits transversely-isotropic symmetry [3]. Therefore, it is assumed that, at all functional length-scale levels, muscle tissue has an identical, incompressible, transversely-isotropic response.

The dynamical process of a continuum model describes the unique kinematical and kinetic state of a material. For materials that exhibit behavior that is dependent on internal processes, such as activation level and actin/myosin cross-bridging in skeletal muscle tissue, the dynamical process can be described using an approach with internal variables [17]. While this approach, commonly used to formulate complex thermodynamics, allows for consideration of changes in heat or mass, the object of the current study is to develop a continuum-based constitutive model to describe the three-dimensional mechanical behavior of muscle under passive and active loading conditions. Following a detailed derivation of the corresponding strain-energy function and constitutive equation, the resulting model is subsequently characterized using modeling data from the literature [9] as a first evaluation of model performance.

Methods

Dyanamical Processes

Consider the reference configuration of a continuous region of skeletal muscle $\mathcal{R}$ with material points X. The passive properties of the effective continuum are modeled as those that result in the same strain-energy density as the actual heterogeneous muscle tissue under identical boundary conditions [18-21]. Likewise, the active properties of the effective continuum are modeled as those that result in the same stress tensor components as the actual muscle tissue under identical applied boundary conditions. It is assumed that isothermal conditions exist and, for the purposes of this model, it is further assumed that the mechanical performance of skeletal muscle is not affected by the transfer of mass or heat across the boundary of $\mathcal{R}$. With these assumptions, the dynamical processes of skeletal muscle can be described by the following functions:

1. The spatial position vector $\mathbf{x} = \chi(X,t)$ in the motion χ
2. The symmetric second Piola-Kirchhoff stress tensor $\mathbf{S} = \mathbf{S}(X,t)$ which is smooth in $\mathbf{x}$
3. The free energy density $\Psi = \Psi(X,t)$
4. The entropy density $\eta = \eta(X,t)$
5. The absolute temperature θ
6. The instantaneous potential energy $U = U(X,t)$
7. The muscle activation $q = q(X,t)$

Functions 1 - 5 have their usual definition [22]. The instantaneous potential energy U $\{U \in \mathbb{R} : U \geq 0\}$ is the energy that is available to increase the amount of actin/myosin overlap.

At the optimal length, U is zero since the overlap is maximized. As the muscle is deformed away from the optimal length (tension or compression), U increases. As the muscle is unloaded from a previously loaded state, this energy is applied to increase the cross-bridging to the level corresponding to the magnitude of deformation (Figure 2). As the muscle length approaches the optimal length, U approaches zero. Therefore, this quantity is the potential energy available to increase the amount of actin-myosin overlap. The activation parameter q $\{q \in \mathbb{R} : 0 \leq q \leq 1\}$ is the amount of activation in the muscle ($q = 1$ for fully activated muscle and $q = 0$ for completely relaxed muscle). The seven functions listed above are a dynamical process in $\mathcal{R}$ if they are compatible with the balance of linear momentum and the balance of energy field equations [22]. In the absence of body forces, the balance of linear momentum is

$$\rho \ddot{\mathbf{x}} = \text{Div } \mathbf{FS} \tag{1}$$

where ρ is the material density with respect to the reference configuration, $\ddot{\mathbf{x}}$ is the acceleration vector, Div is the divergence operator with respect to the reference configuration, and $\mathbf{F}$ is the deformation gradient tensor. For the above-discussed assumptions, the free energy balance is defined as

$$\Psi = \frac{1}{2}\mathbf{S} : \mathbf{C} - U - \theta\eta \tag{2}$$

where $\mathbf{C}$ is the right Cauchy-Green Deformation tensor and a double dot symbol denotes a scalar product of two tensors. The Clasius-Duhem inequality states that the rate of entropy production is non-negative. Using this principle and Equation (2), a functional form of the Clasius-Duhem inequality for an isothermal process is

$$\theta\dot{\eta} = \frac{1}{2}\left(\mathbf{S} : \dot{\mathbf{C}}\right) - U - \dot{\Psi} \geq 0 \tag{3}$$

where a superimposed dot denotes a material derivative. For the current study, it is assumed that the processes described herein are completely reversible, so that no entropy is created. With this assumption, Equation (3) becomes

$$\dot{\Psi} = \frac{1}{2}\left(\mathbf{S} : \dot{\mathbf{C}}\right) - U \tag{4}$$

which is the material derivative of Equation (2) for constant temperature and no entropy production.

Constitutive Modeling

Functions 1-7 represent fourteen scalar fields, which are interrelated by the five field equations, Equations (1), (2), and (4). For a determinate system, nine constitutive equations are required. Consider the following response functions for a given χ and q

$$\Psi = \hat{\Psi}(\mathbf{C}, q)$$
$$\mathbf{S} = \hat{\mathbf{S}}(\mathbf{C}, q)$$
$$\dot{q} = f(\mathbf{C}, q) \tag{5}$$
$$U = \hat{U}(\mathbf{C}, q)$$

where f is a response function and the superimposed caret serves to distinguish response functions from their values. The functional dependencies in Equation (5) are based on the Principle of Equipresence [23, 24], in which a variable present as an independent variable in one constitutive equation is present in all other constitutive equations, unless the contrary is deduced. In this case, there is no physiological reason for the dependence of U on the activation level q. Even when the muscle is not activated, the potential to establish cross-links exists when it is deformed from the optimal length. Therefore, Equation (5)$_4$ is restated as $U = \hat{U}(\mathbf{C})$.

The specific form of $\hat{\Psi}$ is postulated to be

$$\hat{\Psi}(\mathbf{C}, q, \phi) = \Psi_p(\mathbf{C}) + \phi(\mathbf{C})\Psi_a(\mathbf{C}, q) \tag{6}$$

where Ψ_p and Ψ_a are the strain-energy densities associated with the passive and active responses, respectively, of skeletal muscle tissue, and the actin/myosin overlap parameter ϕ {$\phi \in \mathbb{R}$: $0 < \phi \leq 1$} represents the amount of overlap of the actin and myosin fibers such that $\phi = 1$ at the optimized length, and $\phi = 0$ in the situation where no active force generation is possible due to the relative amounts of actin/myosin overlap. The actin/myosin overlap parameter is dependent on the deformation of the muscle. The material derivative of Equation (5)$_1$, with the help of Equations (4) and (6), is

$$\Psi_a(\mathbf{C}, q)\frac{\partial \phi(\mathbf{C})}{\partial \mathbf{C}}:\dot{\mathbf{C}} + \dot{U} = \left[\frac{1}{2}\mathbf{S} - \frac{\partial \Psi_p(\mathbf{C})}{\partial \mathbf{C}} - \phi(\mathbf{C})\frac{\partial \Psi_a(\mathbf{C}, q)}{\partial \mathbf{C}}\right]:\dot{\mathbf{C}} - \phi(\mathbf{C})\frac{\partial \Psi_a(\mathbf{C}, q)}{\partial q}\dot{q} \tag{7}$$

The first term on the left-hand side of Equation (7) is the change in magnitude of free energy due to the changes in the cross–bridging links during deformation. This is apparent from the fact that this is the only term in Equation (7) that has a negative sign during loading from the optimized state, and a positive sign during loading to the optimized state. It is assumed that the magnitude of this term is equal in magnitude, but opposite in sign, to $\dot{U}$. This assumption is motivated by the ability of the curve shown in Figure 2 to be applicable even under repeated loading and unloading of a muscle. No loss of energy occurs in the closed system of the muscle, as indicated by Equation (4), which is based on the assumption of complete reversibility. During a deformation of a muscle, the first two terms in Equation (7) will have opposite signs and equal magnitudes, no matter how the muscle is being deformed from the optimized state. In effect, this assumption establishes the nature and behavior of the term $\dot{U}$. Therefore, under this assumption, the left-hand side of Equation (7) is always zero

$$0 = \left[\frac{1}{2}\mathbf{S} - \frac{\partial \Psi_p(\mathbf{C})}{\partial \mathbf{C}} - \phi(\mathbf{C})\frac{\partial \Psi_a(\mathbf{C},q)}{\partial \mathbf{C}} \right] : \dot{\mathbf{C}} - \phi(\mathbf{C})\frac{\partial \Psi_a(\mathbf{C},q)}{\partial q}\dot{q} \tag{8}$$

Requiring Equation (8) to hold for an arbitrary $\dot{\mathbf{C}}$ and a constant q,

$$\mathbf{S} = 2\left[\frac{\partial \Psi_p(\mathbf{C})}{\partial \mathbf{C}} + \phi(\mathbf{C})\frac{\partial \Psi_a(\mathbf{C},q)}{\partial \mathbf{C}} \right] \tag{9}$$

Taking the following definitions,

$$\mathbf{S}^p \equiv 2\frac{\partial \Psi_p(\mathbf{C})}{\partial \mathbf{C}} \qquad \mathbf{S}^a \equiv 2\phi\frac{\partial \Psi_a(\mathbf{C},q)}{\partial \mathbf{C}} \tag{10}$$

Equation (9) becomes

$$\mathbf{S} = \mathbf{S}^p + \mathbf{S}^a \tag{11}$$

where $\mathbf{S}^p$ and $\mathbf{S}^a$ are the stress tensors associated with the passive and active responses, respectively. The additive decomposition of stress into active and passive components has been previously discussed in the literature [3].

Transversely Isotropic Material Symmetry

Transverse isotropy is characterized by invariance of material properties with respect to arbitrary rotations about a preferred direction $\mathbf{m}_1$ (henceforth referred to as the fiber axis), and reflections from the planes orthogonal to or parallel to the fiber axis. For the current study, the fiber axis is parallel to the orientation of the muscle fibers and myofibrils. The corresponding symmetry group is defined by

$$\mathcal{G} = \left\{ \mathbf{Q} \in \mathrm{Orth} : \mathbf{Q}\mathbf{M}_i\mathbf{Q}^T = \mathbf{M}_i \right\} \tag{12}$$

where Orth represents the set of all orthogonal tensors and $\mathbf{M}_i$ ($i = 1, 2, 3$) are the structural tensors that describes the material symmetry. For transverse isotropic symmetry, the structural tensors are [25]

$$\mathbf{M}_1 = \mathbf{m}_1 \otimes \mathbf{m}_1 \qquad \mathbf{M}_2 = \mathbf{M}_3 = \frac{1}{2}\left(\mathbf{I} - \mathbf{m}_1 \otimes \mathbf{m}_1 \right) \tag{13}$$

where $\mathbf{I}$ is the identity tensor. The condition of transverse isotropic material symmetry is enforced by expressing the strain energy function of Equation (6) in terms of linear combinations of scalar quantities q and ϕ and scalar invariants of $\mathbf{C}$ and $\mathbf{M}_i$. Such scalar invariants of $\mathbf{C}$ and $\mathbf{M}_i$ include [25, 26]

$$I_3 \equiv \det \mathbf{C} = J^2 \qquad J_4 \equiv \mathbf{C}:\mathbf{M}_1 \qquad L_1 \equiv \mathbf{C}:\tilde{\mathbf{M}} \qquad L_2 \equiv \mathbf{C}^{-1}:\tilde{\mathbf{M}} \qquad (14)$$

and

$$\tilde{\mathbf{M}} = \sum_{i=1}^{3} w_i \mathbf{M}_i \qquad (15)$$

where J is the Jacobian (determinant of $\mathbf{F}$) and w_i are weighting factors that dictate the relative difference between properties parallel and orthogonal to the fiber axis and are restricted by $w_1 + w_2 + w_3 = 1$, where $w_2 = w_3$ for transverse isotropy. Therefore, for an orthogonal basis set $e = \{\mathbf{e}_1, \mathbf{e}_2, \mathbf{e}_3\}$ in which $\mathbf{e}_1$ is aligned with $\mathbf{m}_1$, it can be easily shown from Equations (14) and (15) that

$$
\begin{aligned}
I_3 &= \varepsilon_{ijk} C_{1i} C_{2j} C_{3k} \\
J_4 &= C_{11} \\
L_1 &= w_1 C_{11} + w_2 \left(C_{22} + C_{33} \right) \\
L_2 &= \frac{1}{J^2} \left[w_1 \left(C_{22} C_{33} - C_{23}{}^2 \right) + w_2 \left(C_{11} C_{33} + C_{11} C_{22} - C_{13}{}^2 - C_{12}{}^2 \right) \right]
\end{aligned}
\qquad (16)
$$

where ε_{ijk} is the usual permutation symbol. Furthermore, Equation (6) is assumed to have the form

$$\hat{\Psi}(\mathbf{C}, q, \phi) = \Psi_p \left(I_3, L_1, L_2 \right) + \phi(J_4) \Psi_a \left(J_4, q \right) \qquad (17)$$

The specific forms of each term of Equation (17) are discussed below.

Passive Response

While the data available for completely characterizing the 3-dimensional material properties of skeletal muscle tissue are sparse, there are data that suggest that skeletal muscle may have a stiffer response of the muscle in the direction orthogonal to the fiber axis with respect to the direction along the fiber axis [8, 9]. This is contrary to the typical view of transversely isotropic materials, and conventional models of transversely isotropic, hyperelastic materials do not tend to accommodate this peculiarity. In light of this, the modeling of the passive response of skeletal muscle tissue requires a formulation that is capable of handling the case where the higher material stiffness can be in either the fiber axis or orthogonal to that direction. From Equation (16) it can be seen that this difference in stiffnesses can be accommodated through the weighting factors w_i. Thus, it is assumed that the passive component of Equation (17) is

$$\Psi_p \left(I_3, L_1, L_2 \right) = \frac{\mu}{4} \left[\frac{1}{\alpha} \left(L_1{}^{\alpha} - 1 \right) + \frac{1}{\beta} \left(L_2{}^{\beta} - 1 \right) \right] + \frac{p}{2} \left(I_3{}^{1/3} - 1 \right) \qquad (18)$$

where μ, α, and β are material constants $\{\mu, \alpha, \beta \in \mathbb{R}: \mu \geq 0,\ \alpha > 0,\ \beta > 0\}$ and p is an indeterminate Lagrange multiplier for enforcement of the incompressibility constraint $J = 1$. While the first two terms on the right-hand side of Equation (18) were established previously [25], the last term was derived using the typical procedure used for incompressible materials. It is important to note that Equation (18) is polyconvex [27], as demonstrated elsewhere [25, 26]. The polyconvexity condition guarantees the existence of at least one deformation that can be minimized in a standard energy-minimizing technique [26]. From Equation (10)$_1$ the passive component of stress is

$$\mathbf{S}^P = \frac{\mu}{2}\left[\left(L_1^{\alpha-1}\right)\frac{\partial L_1}{\partial \mathbf{C}} + \left(L_2^{\beta-1}\right)\frac{\partial L_2}{\partial \mathbf{C}}\right] + \frac{p}{3}\mathbf{C}^{-1} \tag{19}$$

Further, observing that

$$\frac{\partial}{\partial \mathbf{A}}(\mathbf{A}:\mathbf{B}) = \mathbf{B}$$
$$\frac{\partial}{\partial \mathbf{A}}(\mathbf{A}^{-1}:\mathbf{B}) = -\mathbf{A}^{-1}\mathbf{B}\mathbf{A}^{-1} \tag{20}$$

for arbitrary tensors $\mathbf{A}$ and $\mathbf{B}$ ($\mathbf{A}$ is invertible), Equation (19) becomes

$$\mathbf{S}^P = \frac{\mu}{2}\left[\left(L_1^{\alpha-1}\right)\tilde{\mathbf{M}} - \left(L_2^{\beta-1}\right)\mathbf{C}^{-1}\tilde{\mathbf{M}}\mathbf{C}^{-1}\right] + \frac{p}{3}\mathbf{C}^{-1} \tag{21}$$

Therefore, Equation (21) is the three-dimensional passive stress tensor for the skeletal muscle tissue as a function of material parameters, deformation, and fiber axis orientation.

Active Response

Upon activation, the cross-bridging mechanism in skeletal muscle creates a tensile stress along the fiber axis of the tissue. The amount of tension that the cross-bridging can supply is dependent on the amount of overlap of the actin/myosin filaments. The activated muscle tension is a stress that is superimposed upon the passive stress [3], as shown in Equation (11). It is assumed that the active component of the strain-energy density $\Psi_a(\mathbf{C},q)$ is

$$\Psi_a(\mathbf{C},q) = \frac{1}{2}\gamma q J_4 \tag{22}$$

where γ is a material parameter $\{\gamma \in \mathbb{R}: \gamma \geq 0\}$. The form of Equation (22) is inspired from the expected active response of skeletal muscle tissue [28]. From Equation (10)$_2$ the active component of the stress is

$$\mathbf{S}^a = \gamma q \phi \frac{\partial J_4}{\partial \mathbf{C}} \tag{23}$$

and because

$$\frac{\partial J_4}{\partial \mathbf{C}} = \mathbf{M}_1 \tag{24}$$

Equation (23) is

$$\mathbf{S}^a = \gamma q \phi \mathbf{M}_1 \tag{25}$$

Given that the active response of muscle tissue varies with length as shown in Figure 2, the time-independent evolution of loss in cross-bridging may be captured with

$$\phi = \exp\left[-\frac{\left(J_4 - J_4^0\right)^2}{\left(J_4^0\right)^2} \right] \tag{26}$$

where J_4^0 is the value of J_4 for the optimized cross-bridging condition. Therefore, when $J_4 = J_4^0$, the active component of the stress has a maximum value for a given value of q.

Combined Response

From Equations (17), (18), and (22), the total strain-energy density of skeletal muscle tissue is

$$\hat{\Psi}\left(\mathbf{C}, q, \phi\right) = \frac{\mu}{4}\left[\frac{1}{\alpha}\left(L_1^{\alpha} - 1\right) + \frac{1}{\beta}\left(L_2^{\beta} - 1\right) \right] + \frac{p}{2}\left(I_3^{1/3} - 1\right) + \frac{\gamma}{2}q\phi J_4 \tag{27}$$

From Equations (21) and (25), the constitutive equation for the stress tensor is

$$\mathbf{S} = \frac{\mu}{2}\left[\left(L_1^{\alpha-1}\right)\tilde{\mathbf{M}} - \left(L_2^{\beta-1}\right)\mathbf{C}^{-1}\tilde{\mathbf{M}}\mathbf{C}^{-1} \right] + \frac{p}{3}\mathbf{C}^{-1} + \gamma q \phi \mathbf{M}_1 \tag{28}$$

In the reference configuration, it is assumed that the muscle tissue is undeformed ($\mathbf{C} = \mathbf{I}$), unactivated ($q = 0$), and optimum cross-bridging exists ($\phi = 1$). Under these conditions, the stress from Equation (28) is

$$\mathbf{S}\big|_{\mathbf{C}=\mathbf{I}, q=0, \phi=1} = \mathbf{0} \tag{29}$$

Therefore, Equation (28) appropriately predicts no residual stresses in the muscle tissue in the reference configuration.

12

Model Evaluation

A first evaluation of the current model was characterized through comparisons with the model presented in Jenkyn *et al.* [9] For evaluation of the passive response formulation, the total strain energy density has been determined for both models for three sets of isochoric deformations: a longitudinal extension, a transverse extension, and a longitudinal shear deformation. An additional comparison is made considering the active response functions. Lastly, the responses of a combined active and passive perturbation will be examined. For convenience, the following sections describe the passive and active functions from Jenkyn *et al.* as well as the corresponding specific applications of the current model.

Passive Response

Recall from Equation (21) that the passive mechanical response of skeletal muscle is dependent on four material parameters: μ, α, β, and w_1. The values of these parameters are established by comparing Equation (18) to the two-dimensional passive strain-energy density function developed by. Jenkyn *et. al.* [9]   The passive strain energy for a two-dimensional model of skeletal muscle from the Jenkyn model is

$$\hat{\Psi}^J(\mathbf{E}) = \Psi_1^J(E_{11}) + \Psi_2^J(E_{22}) + \Psi_{12}^J(E_{12}) \tag{30}$$

where $\mathbf{E}$ is the Green strain tensor (henceforth referred to as the strain tensor), $\mathbf{E} = (1/2)(\mathbf{C} - \mathbf{I})$; the fiber axis is parallel to the $\mathbf{e}_1$ basis vector ; and Ψ_1^J, Ψ_2^J, and Ψ_{12}^J are given by

$$\Psi_1^J(E_{11}) = \frac{k}{a_1}\left[\exp(a_1 E_{11}) - a_1 E_{11} - 1\right]$$

$$\Psi_2^J(E_{22}) = \frac{k}{a_2}\left[\exp(a_2 E_{22}) - a_2 E_{22} - 1\right] \tag{31}$$

$$\Psi_{12}^J(|E_{12}|) = \frac{k}{a_{12}}\left[\exp(a_{12}|E_{12}|) - a_{12}|E_{12}| - 1\right]$$

for which k = 50,000 N/m^2, a_1 = 6, a_2 = 8, and a_{12} = 6. To make Equation (31) physically meaningful, it has been modified from what was reported by Jenkyn *et. al.* by adding the term -1 in the brackets such that $\hat{\Psi}^J = 0$ when all strain components are zero-valued, thus satisfying the usual normalization condition for strain-energy functions. Equation (31)$_3$ has been further modified by adding the absolute value operator to the shear strain component E_{12}, thus providing an independence of $\hat{\Psi}^J$ on the sign of the shear strain E_{12}. Additionally, for the purpose of direct comparison with the proposed three-dimensional constitutive formulation, Equation (30) was modified for three dimensions by adding a strain-energy density term $\Psi_3^J(E_{33})$ which describes the response of the material to the strain component E_{33}. The functional form of this added term is

$$\Psi_3^J(E_{33}) = \frac{k}{a_2}\left[\exp(a_2 E_{33}) - a_2 E_{33} - 1\right] \tag{32}$$

This function was chosen so that the response of the material to strain component E_{33} was the same as the material response to strain component E_{22}, because of the transverse isotropy. Strain-energy density terms can be added to Equation (30) corresponding to E_{13} and E_{23} that are similar in form to Equation (31)$_3$, however, these terms have not been added here as they are not necessary for the particular set of applied deformations that are discussed below as E_{13} and E_{23} are zero-valued.

Longitudinal Extension

The motion equations $\mathbf{x} = \chi(X)$ for a longitudinal extension deformation are

$$x_1 = \lambda_1 X_1 \qquad x_2 = \sqrt{1/\lambda_1}\,X_2 \qquad x_3 = \sqrt{1/\lambda_1}\,X_3 \tag{33}$$

where λ_1 $\{\lambda_1 \in \mathbb{R}: \lambda_1 > 0\}$ represents the magnitude of the applied longitudinal extension deformation. This deformation mode is therefore a uniaxial extension parallel to the fiber axis. The corresponding deformation gradient tensor components with respect to the basis set e (described above) is

$$[\mathbf{F}] = [\nabla\chi] = \begin{bmatrix} \lambda_1 & 0 & 0 \\ 0 & \sqrt{1/\lambda_1} & 0 \\ 0 & 0 & \sqrt{1/\lambda_1} \end{bmatrix} \tag{34}$$

where it is easily observed that $J = 1$ for all λ_1. The deformation and strain tensor components are, respectively,

$$[\mathbf{C}] = [\mathbf{F}]^T[\mathbf{F}] = \begin{bmatrix} \lambda_1^2 & 0 & 0 \\ 0 & 1/\lambda_1 & 0 \\ 0 & 0 & 1/\lambda_1 \end{bmatrix} \qquad [\mathbf{E}] = \frac{1}{2}\begin{bmatrix} \lambda_1^2 - 1 & 0 & 0 \\ 0 & (1/\lambda_1) - 1 & 0 \\ 0 & 0 & (1/\lambda_1) - 1 \end{bmatrix} \tag{35}$$

It follows from Equation (16) that

$$\begin{aligned} L_1^{(1)} &= w_1\lambda_1^2 + 2w_2/\lambda_1 \\ L_2^{(1)} &= w_1/\lambda_1^2 + 2w_2\lambda_1 \end{aligned} \tag{36}$$

where the superscripted (1) denotes the deformation associated with λ_1. For the case in which $q=0$, Equation (27) becomes

$$\hat{\Psi}(\mathbf{C}, q, \varsigma) = \frac{\mu}{4} \left\{ \frac{1}{\alpha} \left[\left(w_1 \lambda_1^2 + 2w_2 / \lambda_1 \right)^\alpha - 1 \right] + \frac{1}{\beta} \left[\left(w_1 / \lambda_1^2 + 2w_2 \lambda_1 \right)^\beta - 1 \right] \right\} \qquad (37)$$

Transverse Extension

The motion equations $\mathbf{x} = \chi(X)$ for a transverse extension deformation are

$$x_1 = \left(1/\lambda_2^2 \right) X_1 \qquad x_2 = \lambda_2 X_2 \qquad x_3 = \lambda_2 X_3 \qquad (38)$$

where λ_2 $\{\lambda_2 \in \mathbb{R} : \lambda_2 > 0\}$ represents the magnitude of the applied transverse extension deformation. The corresponding deformation gradient tensor components with respect to the basis set e are

$$[\mathbf{F}] = \begin{bmatrix} 1/\lambda_2^2 & 0 & 0 \\ 0 & \lambda_2 & 0 \\ 0 & 0 & \lambda_2 \end{bmatrix} \qquad (39)$$

where $J = 1$ for all λ_2. The deformation and strain tensor components are

$$[\mathbf{C}] = \begin{bmatrix} 1/\lambda_2^4 & 0 & 0 \\ 0 & \lambda_2^2 & 0 \\ 0 & 0 & \lambda_2^2 \end{bmatrix} \qquad [\mathbf{E}] = \frac{1}{2} \begin{bmatrix} \left(1/\lambda_2^4 \right) - 1 & 0 & 0 \\ 0 & \lambda_2^2 - 1 & 0 \\ 0 & 0 & \lambda_2^2 - 1 \end{bmatrix} \qquad (40)$$

It follows from Equation (16) that

$$L_1^{(2)} = w_1 / \lambda_2^4 + 2w_2 \lambda_2^2$$
$$L_2^{(2)} = w_1 \lambda_2^4 + 2w_2 / \lambda_2^2 \qquad (41)$$

where the superscripted (2) denotes the deformation associated with λ_2. For the case in which $q=0$, Equation (27) becomes

$$\hat{\Psi}(\mathbf{C}, q, \phi) = \frac{\mu}{4} \left\{ \frac{1}{\alpha} \left[\left(w_1 / \lambda_2^4 + 2w_2 \lambda_2^2 \right)^\alpha - 1 \right] + \frac{1}{\beta} \left[\left(w_1 \lambda_2^4 + 2w_2 / \lambda_2^2 \right)^\beta - 1 \right] \right\} \qquad (42)$$

Longitudinal Shear

The motion equations $\mathbf{x} = \chi(X)$ for a longitudinal shear deformation are

$$x_1 = X_1 + \lambda_3 X_2 \qquad x_2 = X_2 \qquad x_3 = X_3 \tag{43}$$

where λ_3 $\{\lambda_3 \in \mathbb{R}: \lambda_3 > 0\}$ represents the magnitude of the applied longitudinal shear deformation. This deformation corresponds to shearing in a plane parallel to the fiber axis. The corresponding deformation gradient tensor components with respect to the basis set e are

$$[\mathbf{F}] = \begin{bmatrix} 1 & \lambda_3 & 0 \\ 0 & 1 & 0 \\ 0 & 0 & 1 \end{bmatrix} \tag{44}$$

where $J = 1$ for all λ_3. The deformation and strain tensor components are

$$[\mathbf{C}] = \begin{bmatrix} 1 & \lambda_3 & 0 \\ \lambda_3 & 1+\lambda_3^2 & 0 \\ 0 & 0 & 1 \end{bmatrix} \qquad [\mathbf{E}] = \frac{1}{2} \begin{bmatrix} 0 & \lambda_3 & 0 \\ \lambda_3 & \lambda_3^2 & 0 \\ 0 & 0 & 0 \end{bmatrix} \tag{45}$$

It follows from Equation (16) that

$$L_1^{(3)} = w_1 + w_2 \left(2 + \lambda_3^2 \right)$$
$$L_2^{(3)} = w_1 \left(1 + \lambda_3^2 \right) + 2w_2 \tag{46}$$

where the superscripted (3) denotes the deformation associated with λ_3. For the case in which $q=0$, Equation (27) becomes

$$\hat{\Psi}(\mathbf{C},q,\phi) = \frac{\mu}{4} \left\{ \frac{1}{\alpha} \left[\left(w_1 + 2w_2 + w_2 \lambda_3^2 \right)^{\alpha} - 1 \right] + \frac{1}{\beta} \left[\left(w_1 + w_1 \lambda_3^2 + 2w_2 \right)^{\beta} - 1 \right] \right\} \tag{47}$$

Active Response

Recall that the active mechanical response of skeletal muscle is dependent on two material parameters: γ and J_4^0. The values of the parameters have been established by comparing Equation (25) to the active stress given by the Jenkyn model [9] which was originally established by Hill [2], given by

$$\mathbf{S}_J^a = q(SF)M(E_{11}) \tag{48}$$

where $SF = 225,000$ N/m^2 [29, 30] and

$$M\left(E_{11}\right) = \begin{cases} \exp\left(b_1 E_{11}{}^3\right) & E_{11} \le 0 \\ \exp\left(b_2 E_{11}{}^2\right) & E_{11} > 0 \end{cases} \qquad (49)$$

In Equation (49), $b_1 = 10$ and $b_2 = -6$. An iterative least squares analysis was used to minimize the error between the current model and the Jenkyn model for a range of E_{11} values of $(-0.3 \le E_{11} \le 1.3)$ under conditions of full muscle activation ($q = 1$) for the longitudinal extension (section 8.1). This range was chosen based on the longitudinal extension range used in the previous sections.

Combined Passive/Active Response

To demonstrate the predicted skeletal muscle response with both active and passive components of stress, a longitudinal extension was applied to the model with $q = 1$. From Equations (15), (28), (33), (35), and (36) the S_{11} component of stress is

$$S_{11} = \frac{\mu}{2}\left[w_1\left(w_1\lambda_1{}^2 + 2w_2/\lambda_1\right)^{\alpha-1} - w_1\lambda_1{}^{-4}\left(w_1/\lambda_1{}^2 + 2w_2\lambda_1\right)^{\beta-1}\right] + \gamma q\phi \qquad (50)$$

For the Jenkyn model, the same component of stress is [9]

$$S_{11}^J = \frac{k}{a_1}\left[a_1 \exp\left(a_1 E_{11}\right) - a_1\right] + q(SF)M\left(E_{11}\right) \qquad (51)$$

Results

Passive Response

The parameters μ, α, β, and w_1 were determined by directly comparing strain-energy densities from the current model and the model of Jenkyn *et. al.* [9] . For all three sets of deformations described above, an iterative least-squares procedure was used to minimize the error between the two models for ranges of deformations of $0.632 \le \lambda_1 \le 1.897$, $0.632 \le \lambda_2 \le 1.897$, and $0.632 \le \lambda_3 \le 1.897$ corresponding to the applied strains of $-0.3 \le E_{11} \le 1.3$, $-0.3 \le E_{22} = E_{33} \le 1.3$, and $-0.3 \le E_{12} \le 0.3$, respectively, with the unidentified strain components determined using Equations $(35)_2$, $(40)_2$, and $(45)_2$, respectively. The range of deformations for the longitudinal extension case was based on experimental data for tension [28] and the kinematics constraints for incompressible materials in compression. The range of deformation of the transverse extension case was chosen to match the strain for the longitudinal extension case. Lacking empirical data the range of strain for the longitudinal shear case was chosen based on the expected longitudinal shear strains in skeletal muscle tissue. The comparisons of strain-energy densities for each of the three deformations over corresponding ranges of deformations are shown in Figures 3 – 5. The resulting values from the least-squares analysis of the material parameters are

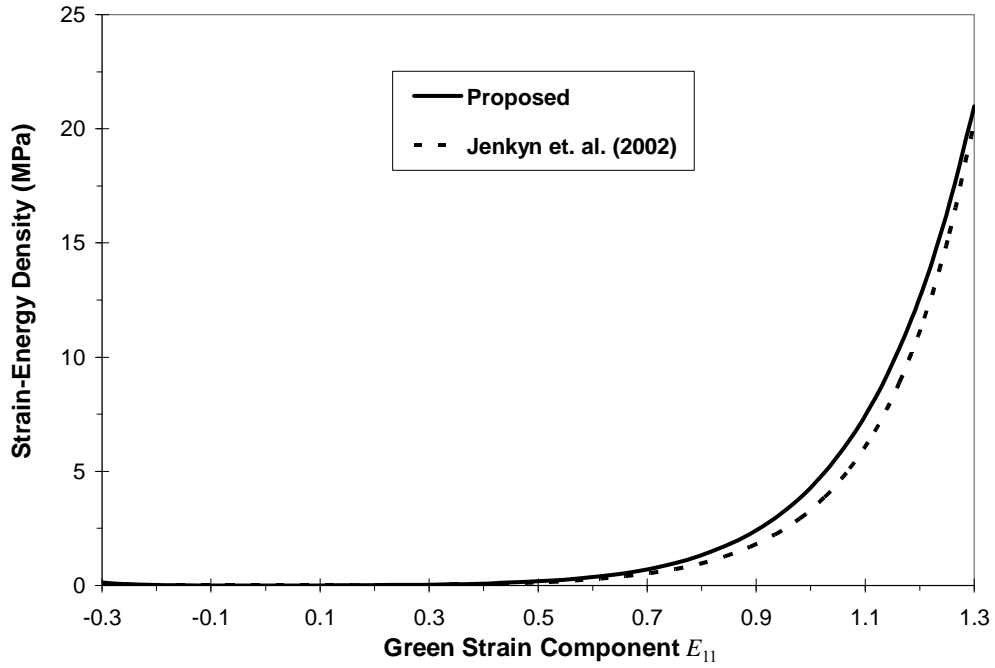$$\mu = 300 \text{ kPa} \quad \alpha = 11.1 \quad \beta = 5.3 \quad w_1 = 0.5 \qquad (52)$$

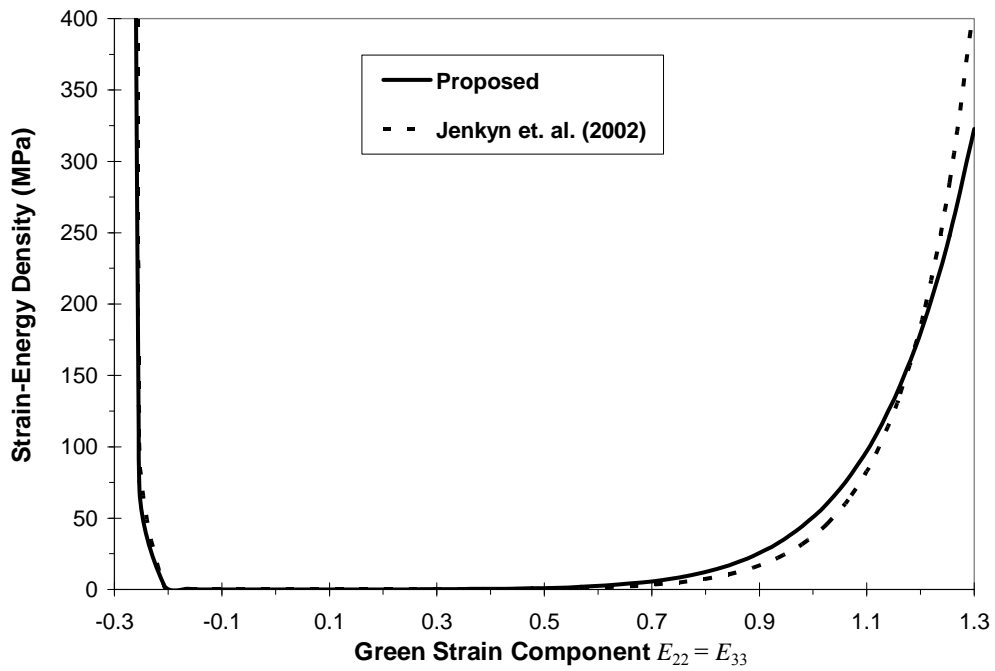*Figure 3. Strain-energy density for passive longitudinal extension deformation*

Figure 4. Strain-energy density for passive transverse extension deformation
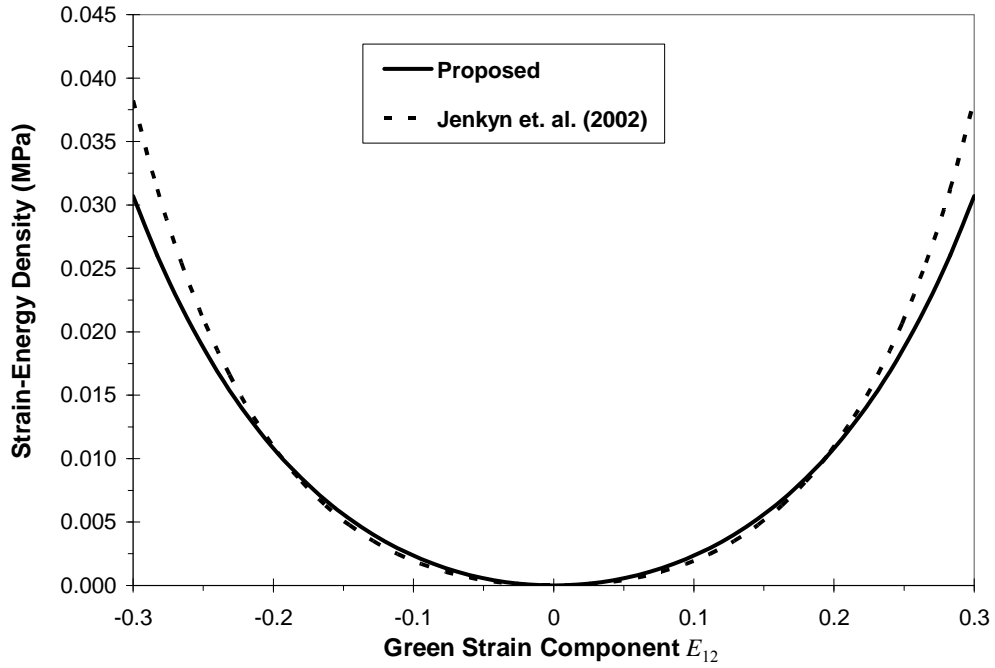
Figure 5. Strain-energy density for passive longitudinal shear deformation
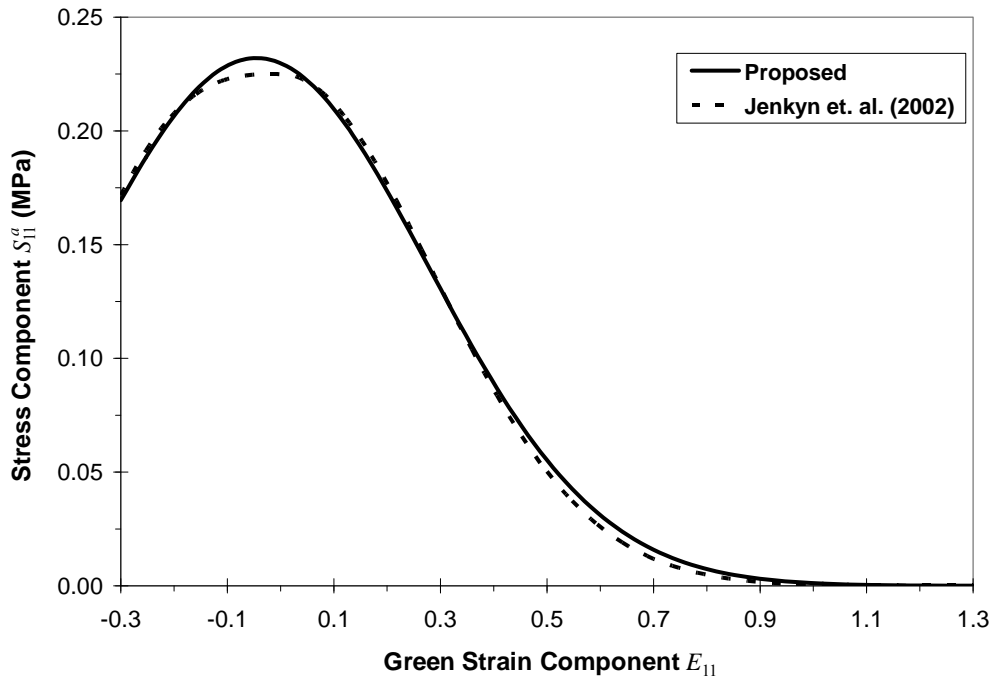

Figure 6. Active stress versus strain diagram for fully activated skeletal muscle

It is important to note that longitudinal-shear loading condition consists of a shear-dominated combined loading in order to maintain the incompressible kinematic constraint for large deformations. It is also important to note that the Lagrange multiplier p cannot be evaluated from the above-described loading conditions, since they are isochoric deformations. The Lagrange multiplier is necessary when using the proposed constitutive model under more complex loading conditions, as is often performed in finite element modeling. The value of this parameter does not necessarily reflect the material response, and is thus not a unique material parameter. In fact, standard routines are used to adjust this parameter in finite element analyses to enforce incompressibility [31]. Because the current study is only concerned with simple isochoric deformations of a volume of muscle for the purposes of constitutive modeling development, a full structural analysis of muscle tissue under complex loadings has not been performed. Therefore, it is out of the scope of this paper to analyze the behavior of the Lagrange multiplier for a full muscle subjected to loads.

Active Response

The resulting values of the parameters are

$$\gamma = 232 \text{ kPa}$$
$$J_4^0 = 0.91$$

(53)

A comparison of the active stress component S_{11}^a for the two models using these parameters is shown in Figure 6.

Combined Passive/Active Response

A comparison of the total stress response for the two models is shown in Figure 7 for the range of longitudinal strains of $-0.3 \leq E_{11} \leq 1.3$. This range was chosen for consistency with the strains used in the previous sections. The inset of Figure 7 is the small-strain region of the plot. The nonlinearity of the data in the small-strain region resembles the expected combined response sketched in Figure 2. An inflection point exists at $E_{11} \approx 0.1$ where the active tension is decreasing and the passive tension is increasing with increasing E_{11}.

Discussion

The passive response predicted by the proposed model (Figs. 3 – 5) shows excellent agreement with the response predicted by the Jenkyn model for the three passive deformations. Similarly, the active response also shows excellent agreement between the two models, as demonstrated in Figure 6. Likewise, as one might expect from these results, the combined passive and active stresses for the longitudinal extension show excellent agreement (Fig. 7). The lack of a single comprehensive set of empirical data for the described deformation modes (active longitudinal, passive longitudinal, passive transverse, and passive shear deformations) makes it difficult to assess the accuracy of the predicted behavior of the two models. Qualitatively, the predicted behavior for the individual deformation modes exhibits the expected trends. In that the other existent model do not characterize muscle in either transverse elongation or longitudinal shear,

the Jenkyn model appears to be the most comprehensive model for skeletal muscle tissue currently available in the literature in that it incorporates all of the deformation modes listed above, albeit in two dimensions. Therefore, in the absence of an experimental validation, the results from this first evaluation indicate that the predicted behavior from the proposed model agrees with the expected behavior and with the most comprehensive model currently available for skeletal muscle tissue.
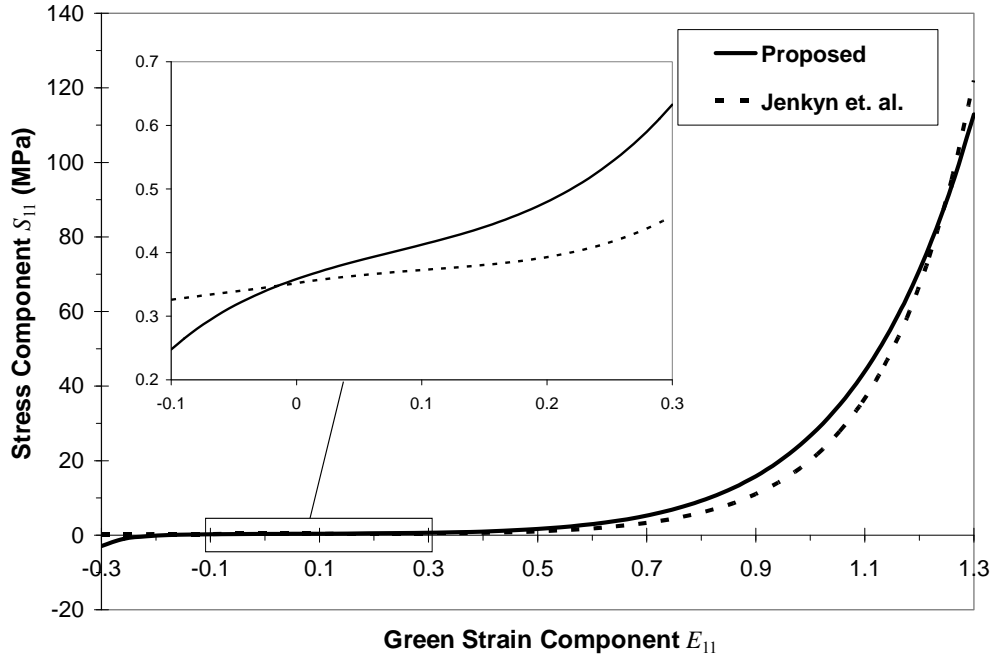
Figure 7. Total stress versus strain diagram for fully activated skeletal muscle. The inset is the small-strain region. The nonlinearity of the data in the small-strain region is consistent with the expected physiological response (see Figure 2). An inflection point exists at E_{11}~0.1 where the active tension is decreasing and the passive tension is increasing.

It is also important to note that the proposed model has been characterized for specific ranges of deformation in the current study. These ranges were chosen based on the entire ranges of deformations that are physiologically realizable for *in vivo* skeletal muscle. Alternatively, the model can be characterized for different sub-sets of these strain ranges, based on the regions of interest for specific muscles, further improving the model's accuracy.

The proposed model has achieved three important goals. First, the model has been developed to describe the incompressible response of skeletal muscle tissue under any three-dimensional, isochoric deformation. This is evident in viewing Equations (27) and (28), which are formulated using three-dimensional stress and deformation tensors. Expanding the formulation to three-dimensions is a necessary step for modeling muscles with complex geometries and is a distinct improvement over previous two-dimensional models [8, 9].

Second, the proposed model is formulated in terms of both the strain energy and stress tensor for both passive and active responses, as shown in Equations (27) and (28). Previous models for skeletal muscle tissue have explicitly modeled the active response in terms of stress only [8-14], leaving the strain-energy density function defined as partial derivative with respect to strain. This makes the formulation dependent upon the deformation of the tissue and would necessitate recalculation of the strain-energy density for each deformation in a proposed analysis. The approach taken with the current model allows the strain-energy density and stress tensor components to be easily and directly evaluated throughout skeletal muscle tissue during any deformation, without integration of the stress function. For this reason, it is anticipated that use of such a formulation will easily lend itself to computational simulation of skeletal muscles *in vivo*, given the complex anatomical paths and interactions with surrounding tissues (e.g., contact with bone and other muscles).

Third, this approach, in particular the use of the dynamical formulation approach, is particularly useful for incorporating the effects of muscle fatigue and damage [32, 33] on the mechanical response of muscle. Because the current study focuses on the development of the constitutive modeling framework, the influence of factors such as fatigue and muscle damage were not addressed herein. This modeling approach was specifically designed to be able to allow for the future incorporation of these processes that occur in biological tissue. A dynamical approach, with an explicit strain-energy density function and open framework will allow for modifying terms to be added. While the effects of damage and heat transfer in constitutive models have not previously been examined in this manner in muscle, examples illustrating the modeling of these pheonomena in other materials are available [34-38]. With this type of approach, the influence of outside factors can be easily incorporated into constitutive equations by modifying the strain energy expressions, which are scalar. Otherwise, the influence of outside factors must be incorporated into the stress-strain relationships via tensoral functions. Modeling the influence of outside influences with scalar functions is more efficient than with tensoral functions, usually will little loss of generality.

Finally, it bears mentioning that any developed constitutive model cannot be fully evaluated until it is compared against experimental data. As mentioned previously, there is a dearth of experimentation of muscle material properties in transverse elongation and shear. Experiments (i.e., load-elongation tests of longitudinal and transverse extension, and longitudinal shear) are currently being performed to generate a comprehensive set of tensile material properties from which material parameters for the current model may be determined.

Summary

A model for predicting the mechanical response of skeletal muscle tissue under both active and passive conditions has been proposed. The model has be developed to describe the mechanical behavior for any isochoric, three-dimensional deformation by predicting the passive and active stresses and strain-energy densities for any point in the motion of the muscle.

The proposed model has been characterized through comparison with a previously-published model for skeletal muscle tissue [9] for the following deformations: passive extension along the fiber axis, passive extension transverse to the fiber axis, passive shear, active extension along the

fiber axis, and combined passive and active extension along the fiber axis. While the resulting material parameters are based on a large range of possible deformations, the model can also be characterized for limited deformation ranges with improved accuracy pending the availability of suitable empirical data. A comparison of the characterized proposed model and the Jenkyn model indicates a general agreement in predicted response to the above-mentioned deformations.

Acknowledgements

References

[1]   Blix, M., 1894, "Die Langrund dei Spennung des Muskels," Skand Arch Physiol, 5, pp. 149-206.
[2]   Hill, A. V., 1938, "The Heat of Shortening and the Dynamic Constants of Muscle," Proceedings of the Royal Society of London, Series B, 126, pp. 136-195.
[3]   Zajac, F. E., 1989, "Muscle and Tendon: Properties, Models, Scaling, and Application to Biomechanics and Motor Control," Critical Reviews in Biomedical Engineering, 17(4), pp. 359-411.
[4]   Delp, S. L., and Loan, J. P., 1995, "A Graphics-Based Software System to Develop and Analyze Models of Musculoskeletal Structures," Computers in Biology and Medicine, 25(1), pp. 21-34.
[5]   Kaufman, K. R., An, K. W., Litchy, W. J., and Chao, E. Y., 1991, "Physiology Prediction of Muscle Forces-I: Theoretical Formulation," Neuroscience, 40(3), pp. 781-792.
[6]   Buchanan, T. S., Lloyd, D. G., Manal, K., and Besier, T. F., 2005, "Estimation of Muscle Forces and Joint Moments Using a Forward-Inverse Dynamics Model," Medicine & Science in Sports & Exercise, 37(11), pp. 1911-1916.
[7]   Van der Linden, B. J. J. J., Koopman, H. F. J. M., Huijing, P. A., and Grootenborer, H. J., 1998, "Revised Planimetric Model of Unipennate Skeletal Muscle: A Mechanical Approach," Clinical Biomechanics, 13(4-5), pp. 256-260.
[8]   Van der Linden, B. J. J. J., 1998, "Mechanical Modeling of Skeletal Muscle Functioning," University of Twente, The Netherlands.
[9]   Jenkyn, T. R., Koopman, B., Huijing, P., Lieber, R. L., and Kaufman, K. R., 2002, "Finite Element Model of Intramuscular Pressure During Isometric Contraction of Skeletal Muscle," Physics in Medicine and Biology, 47, pp. 4043-4061.
[10]   Martins, J. A. C., Pires, E. B., Salvado, R., and Dinis, P. B., 1998, "A Numerical Model of Passive and Active Behavior of Skeletal Muscles," Computer Methods in Applied Mechanics and Engineering, 151, pp. 419-433.
[11]   Gielen, A. W. J., Oomens, C. W. J., Bovendeerd, P. H. M., Arts, T., and Janssen, J. D., 2000, "A Finite Element Approach for Skeletal Muscle using a Distributed Moment Model of Contraction," Computer Methods in Biomechanics and Biomedical Engineering, 3, pp. 231-244.
[12]   Johansson, T., Meier, P., and Blickman, R., 2000, "A Finite-Element Model for the Mechanical Analysis of Skeletal Muscles," Journal of Theoretical Biology, 206, pp. 131-149.
[13]   Yucesoy, C. A., Koopman, B., Huijing, P. A., and Grootenboer, H. J., 2002, "Three-Dimensional Finite Element Modeling of Skeletal Muscle Using a Two-Domain Approach: Linked Fiber-Matrix Mesh Model," Journal of Biomechanics, 35, pp. 1253-1262.

[14]   Blemker, S. S., Pinsky, P. M., and Delp, S., 2005, "A 3D Model of Muscle Reveals the Causes of Nonuniform Strains in the Biceps Brachii," Journal of Biomechanics, 38, pp. 657-665.

[15]   McMahon, T. A., 1984, Muscles, Reflexes, and Locomotion, Princeton University Press, Princeton, NJ.

[16]   Cobb, M., 2002, "Timeline: Exorcizing the Animal Spirits: Jan Swammerdam on Nerve Function," Nature Reviews Neuroscience, 3(5), pp. 395-400.

[17]   Coleman, B. D., and Gurtin, M. E., 1967, "Thermodynamics with Internal State Variables," Journal of Chemical Physics, 47(2), pp. 597-613.

[18]   Valavala, P. K., Clancy, T. C., Odegard, G. M., and Gates, T. S., 2007, "Nonlinear Multiscale Modeling of Polymer Materials," International Journal of Solids and Structures, 44(3-4), pp. 1161-1179.

[19]   Hill, R., 1963, "Elastic Properties of Reinforced Solids: Some Theoretical Principles," Journal of the Mechanics and Physics of Solids, 11, pp. 357-372.

[20]   Hashin, Z., and Rosen, B. W., 1964, "The Elastic Moduli of Fiber-Reinforced Materials," Journal of Applied Mechanics, 31, pp. 223-232.

[21]   Noor, A. K., 1988, "Continuum Modeling for Repetitive Lattice Structures," Applied Mechanics Reviews, 41(7), pp. 285-296.

[22]   Truesdell, C., and Noll, W., 2004, The Non-Linear Field Theories of Mechanics, Springer-Verlag, New York.

[23]   Truesdell, C. A., and Toupin, R. A., 1960, "The Classical Field Theories," Encyclopedia of Physics, Volume III/1: Principals of Classical Mechanics and Field Theory, S. Flugge, ed., Springer-Verlag, Berlin, Germany.

[24]   Eringen, A. C., 1967, Mechanics of Continua, John Wiley & Sons, Inc., New York.

[25]   Itskov, M., and Aksel, N., 2004, "A Class of Orthotropic and Transversely Isotropic Hyperelastic Constitutive Models Based on a Polyconvex Strain Energy Function," International Journal of Solids and Structures, 41, pp. 3833-3848.

[26]   Schroder, J., and Neff, P., 2003, "Invariant Formulation of Hyperelastic Transverse Isotropy Based on Polyconvex Free Energy Functions," International Journal of Solids and Structures, 40, pp. 401-445.

[27]   Ball, J. M., 1977, "Convexity Conditions and Existence Theorems in Nonlinear Elasticity," Archive for Rational Mechanics and Analysis, 63, pp. 337-403.

[28]   Leiber, R. L., 2002, Skeletal Muscle Structure, Function, & Plasticity: The Physiological Basis of Rehabilitation, Lippincott Williams & Wilkins, New York.

[29]   Powell, P. L., Roy, R. R., Kanim, P., Bello, M. A., and Edgerton, V. R., 1984, "Predictability of Skeletal Muscle Tension from Architectural Determinations in Guinea Pig Hindlimbs," Journal of Applied Physiology, 57(6), pp. 1715-1721.

[30]   Fukunaga, T., Roy, R. R., Shellock, F. G., Hodgson, J. A., and Edgerton, V. R., 1996, "Specific Tension of Human Plantar Flexors and Dorsiflexors," Journal of Applied Physiology, 80(1), pp. 158-165.

[31]   Bathe, K. J., 1996, Finite Element Procedures, Prentice-Hall, Inc., Englewood Cliffs, NJ.

[32]   Butterfield, T. A., and Herzog, W., 2005, "Quantification of muscle fiber strain during in vivo repetitive stretch-shortening cycles," Journal of Applied Physiology, 99(2), pp. 593-602.

[33]   Butterfield, T. A., and Herzog, W., 2006, "Effect of altering starting length and activation timing of muscle on fiber strain and muscle damage," Journal of Applied Physiology, 100(5), pp. 1489-1498.

[34]   Talreja, R., 1990, "Internal Variable Damage Mechanics of Composite Materials," Yielding, Damage, and Failure of Anisotropic Solids, J. P. Boehler, ed., Mechanical Engineering Publications, London, pp. 509-533.

[35]   Voyiadjis, G. Z., and Kattan, P. I., 1994, "Micromechanical Modeling of Damage and Plasticity in Continuously Reinforced MMCs," Inelasticity and Micromechanics of Metal Matrix Composites, G. Z. Voyiadjis, and J. W. Ju, eds., Elsevier, Kidlington, UK.

[36]   Ladeveze, P., 1994, "Inelastic Strains and Damage," Damage Mechanics of Composite Materials, R. Talreja, ed., Elsevier, Kidlington, UK.

[37]   Ju, J. W., 1990, "Isotropic and Anisotropic Damage Variables in Continuum Damage Mechanics," Journal of Engineering Mechanics, 116(12), pp. 2764-2770.

[38]   Allen, D. H., Harris, C. E., and Groves, S. E., 1987, "A Thermomechanical Constitutive Theory for Elastic Composites with Distributed Damage - I. Theoretical Development," International Journal of Solids and Structures, 23(9), pp. 1301-1318.